Serveur Académique Lausannois SERVAL serval.unil.ch

Author Manuscript
Faculty of Biology and Medicine Publication

This paper has been peer-reviewed but dos not include the final publisher proof-corrections or journal pagination.

Published in final edited form as:

Title: HDLs protect the MIN6 insulinoma cell line against tunicamycin-induced apoptosis without inhibiting ER stress and without restoring ER functionality.
Authors: Puyal J, Pétremand J, Dubuis G, Rummel C, Widmann C
Journal: Molecular and cellular endocrinology
Year: 2013 Dec 5
Volume: 381
Issue: 1-2
Pages: 291-301
DOI: 10.1016/j.mce.2013.08.016

In the absence of a copyright statement, users should assume that standard copyright protection applies, unless the article contains an explicit statement to the contrary. In case of doubt, contact the journal publisher to verify the copyright status of an article.

serval
serveur académique lausannois

UNIL | Université de Lausanne
Faculté de biologie
et de médecine

Accepted Manuscript

HDLs protect the MIN6 insulinoma cell line against tunicamycin-induced apoptosis without inhibiting ER stress and without restoring ER functionality

Julien Puyal, Jannick Pétremand, Gilles Dubuis, Coralie Rummel, Christian Widmann

PII: S0303-7207(13)00353-5
DOI: http://dx.doi.org/10.1016/j.mce.2013.08.016
Reference: MCE 8621

To appear in: Molecular and Cellular Endocrinology Molecular and Cellular Endocrinology

Received Date: 2 April 2013
Revised Date: 22 August 2013
Accepted Date: 22 August 2013

Please cite this article as: Puyal, J., Pétremand, J., Dubuis, G., Rummel, C., Widmann, C., HDLs protect the MIN6 insulinoma cell line against tunicamycin-induced apoptosis without inhibiting ER stress and without restoring ER functionality, Molecular and Cellular Endocrinology Molecular and Cellular Endocrinology (2013), doi: http://dx.doi.org/10.1016/j.mce.2013.08.016

This is a PDF file of an unedited manuscript that has been accepted for publication. As a service to our customers we are providing this early version of the manuscript. The manuscript will undergo copyediting, typesetting, and review of the resulting proof before it is published in its final form. Please note that during the production process errors may be discovered which could affect the content, and all legal disclaimers that apply to the journal pertain.

ACCEPTED MANUSCRIPT

HDLs protect the MIN6 insulinoma cell line against tunicamycin-induced apoptosis without inhibiting ER stress and without restoring ER functionality

Julien Puyal*[2], Jannick Pétremand*[1], Gilles Dubuis*[1], Coralie Rummel[2], Christian Widmann[1]

[1] Department of Physiology and [2]Department of Fundamental Neurosciences, University of Lausanne, Switzerland

* Equal contribution

Correspondence to Christian Widmann, Department of Physiology, Bugnon 7, 1005 Lausanne, Switzerland, Phone: +41 21 692 5123, Fax: +41 21 692 5505, E-mail: Christian.Widmann@unil.ch.

ACCEPTED MANUSCRIPT

Abstract

HDLs protect pancreatic beta cells against apoptosis induced by several endoplasmic reticulum (ER) stressors, including thapsigargin, cyclopiazonic acid, palmitate and insulin over-expression. This protection is mediated by the capacity of HDLs to maintain proper ER morphology and ER functions such as protein folding and trafficking. Here, we identified a distinct mode of protection exerted by HDLs in beta cells challenged with tunicamycin (TM), a protein glycosylation inhibitor inducing ER stress. HDLs were found to inhibit apoptosis induced by TM in the Min6 insulinoma cell line and this correlated with the maintenance of a normal ER morphology. Surprisingly however, this protective response was neither associated with a significant ER stress reduction, nor with restoration of protein folding and trafficking in the ER. These data indicate that HDLs can use at least two mechanisms to protect beta cells against ER stressors. One that relies on the maintenance of ER function and one that operates independently of ER function modulation. The capacity of HDLs to activate several anti-apoptotic pathways in beta cells may explain their ability to efficiently protect these cells against a variety of insults.

Key words: HDL; endoplasmic reticulum; apoptosis; pancreatic beta cell; tunicamycin

ACCEPTED MANUSCRIPT

1. Introduction

Low HDL level in the blood is an independent risk factor of developing diabetes (Rohrer et al., 2004; von Eckardstein et al., 2000). This indicates that HDLs have beneficial effects on the insulin-producing pancreatic beta cells and/or on the peripheral tissues that respond to insulin. Indeed, studies performed in humans indicate that HDLs increase beta cell insulin secretory function and glucose utilization of muscle cells (Drew et al., 2009). The beneficial effects of HDLs on beta cells are multiple. They increase their insulin secretory capacity (Fryirs et al., 2010) and they protect them against apoptosis induced by a variety of stress and noxious stimuli, including oxidized LDLs (Abderrahmani et al., 2007; Cnop et al., 2002), starvation (Petremand et al., 2009), inflammatory cytokines (Petremand et al., 2009; Rutti et al., 2009), and ER stress (Petremand et al., 2009; Petremand et al., 2012; Rutti et al., 2009).

The HDL-mediated protective mechanisms have been investigated in details in endothelial cells. HDL-mediated signaling in endothelial cells can occur through binding to the lipoprotein receptor scavenger receptor class B member I (SR-BI) and activation of G protein-coupled receptors of the Edg family that bind to sphingosine-1-phosphate molecules carried by HDL particles (Al-Jarallah and Trigatti, 2010; Kimura et al., 2010; Nofer et al., 2004). Incubation of endothelial cells with HDL leads to activation of the Akt anti-apoptotic kinase (Nofer et al., 2001). Although not formally demonstrated, stimulation of the SR-BI/Edg signaling pathway is believed to mediate Akt activation in HDL-stimulated endothelial cells. The anti-apoptotic pathways activated by HDLs in pancreatic beta cells appear different. There is currently no evidence that HDLs activate Akt in beta cells. Additionally, SR-BI does not participate in HDL-mediated beta cell protection (Petremand et al., 2012; Rutti et al., 2009; von Eckardstein and Sibler, 2011).

Pancreatic beta cells rely on their extensively developed ER to fulfill their main function which is to secrete insulin. If ER homeostasis is perturbed, for example as a result of increased insulin secretion demand or in response to free fatty acids (e.g. palmitate), ER stress ensues and this can lead to beta cell apoptosis, and eventually, in vivo, to diabetes development (Eizirik et al., 2008; Eizirik and Cnop, 2010).

ACCEPTED MANUSCRIPT

The unfolded protein response is induced physiologically by cells experiencing ER stress. The goal of this response is to restore ER homeostasis. This is mediated by diminishing the ER load by reducing protein synthesis and by increasing the folding capacity of the ER and the degradation of misfolded protein. If despite these responses ER homeostasis cannot be achieved, the UPR activates pro-apoptotic pathways so that the cells with malfunctioning ER are eliminated. The UPR consists in the activation of three different signaling arms that regulate distinct as well as overlapping set of genes (reviewed in (Hetz, 2012). These different pathways are stimulated when three ER-located proteins, inositol-requiring protein 1 (IRE1), activating transcription factor 6 (ATF6), and protein kinase RNA-like ER kinase (PERK) become activated upon ER stress. Activated IRE1 induces the splicing of the XBP1 mRNA so that it encodes a functional transcription factor. IRE1 can also lead to the stimulation of the JNK MAPK pathway. PERK is a kinase that phosphorylates the initiation factor eukaryotic translation initiator factor 2α (eIF2α), which is then hampered in its capacity to mediate global translation but which at the same time acquires the ability to mediate the translation of a few selected proteins such as ATF4. Finally, ATF6 is a transcription factor that moves from the ER to the Golgi where it is activated by cleavage and then translocates to the nucleus. The UPR regulates genes encoding BiP, a protein chaperone and CHOP, a pro-apoptotic transcription factor (Hetz, 2012)

Recently, the capacity of HDLs to inhibit apoptosis induced by ER stressors such as palmitate or the SERCA inhibitor thapsigargin (TG) has been attributed to their ability to preserve normal morphology and functionality of the ER (Petremand et al., 2012). In particular, HDLs permit beta cells to maintain normal protein folding in the ER and correct protein trafficking through this organelle despite the presence of ER stressors (Petremand et al., 2012). Here we show that HDLs are able to inhibit apoptosis of beta cells induced by tunicamycin, a protein glycosylation inhibitor, known to induce ER stress (Petremand et al., 2009). Surprisingly, this protection was neither associated with a reduction in ER stress nor with restoration of protein folding and trafficking in the ER. There are therefore situations where HDLs inhibit ER stress-induced apoptosis in conditions where the ER stress is not alleviated. This indicates that HDLs can use alternative ways than preservation of ER function to protect beta cells facing ER stress.

ACCEPTED MANUSCRIPT

2. Materials and Methods

2.1. Chemicals

Tunicamycin and thapsigargin were purchased from Sigma (catalog n°T7765 and T9033, respectively). The nondenaturing Zwitterionic detergent 3-[(3-cholamidopropyl)dimethylammonio]-1 propanesulfonate (CHAPS) was from Fluka (catalog n°26680). Palmitate was prepared as described earlier (Petremand et al., 2012).

2.2. Cell culture

The MIN6B1 mouse insulinoma cell line (referred here as MIN6) was maintained in DMEM, 25 mM glucose, supplemented with 15% fetal calf serum (FCS), 1% sodium pyruvate, 83 µM β-mercaptoethanol. In experiments using MIN6, cells were plated in six-well plates at a density of 0.5 million cells per well and cultured for 2 days before treatment; alternatively, when glass cover slips were added in the six-well plates, 0.3 million cells were seeded per well and cultured for 3 days before treatments.

2.3. Western Blot

Insulinoma cells were lysed in monoQ-c [70 mM β-glycerophosphate, 0.5% Triton X-100, 2 mM $MgCl_2$, 1 mM EGTA, 100 µM Na_3VO_4, 1 mM dithiothreitol, 20 µg/ml aprotinin, complete EDTA-free Protease Inhibitor Cocktail Tablets (Roche; 1 tablet per 50 ml) and incubated 15 minutes on ice. The lysate was spun in an Eppendorf centrifuge for 10 minutes at full speed at 4°C and the cleared lysate was then recovered.

Proteins were separated on SDS-PAGE and blotted onto nitrocellulose membranes (BioRad, catalog n°1620115). Thereafter, membranes were incubated in TBS (18 mM HCl, 130 mM NaCl, 20 mM Tris), 0.1% Tween 20 (Acros Organics; catalog n°233362500) (TBS-T) and 5% milk (v:v) for one hour at room temperature and then incubated overnight with the appropriate primary antibody.

ACCEPTED MANUSCRIPT

The primary antibodies used in TBS-T 5% milk were the following: anti-CHOP (Santa Cruz; catalog n°7351) diluted 1:500, anti-actin (Cell Signaling, catalog n° 4968) diluted 1:5000, anti-Bax (N-20 from Santa Cruz, catalog n°493 diluted 1/1000.

The following primary antibodies were all diluted 1:1'000 (unless otherwise indicated) in TBS-T containing 5% BSA (v:v): anti-BiP (=GRP78, Santa Cruz, catalog n°13968) diluted 1:500, anti-caspase-3 (Cell Signaling, catalog n°9661), anti-phospho-PERK (Cell Signaling, catalog n° 3179), anti phospho-Akt mouse monoclonal antibody (Ser473) (Cell Signaling, catalog n° 4051), anti phospho-SAPK/JNK (Thr183/Tyr185) rabbit polyclonal antibody (Cell Signaling, catalog n° 9251), anti-pan Akt rabbit monoclonal 11E7 antibody (Cell Signaling, catalog n° 4685), and anti-SAPK/JNK rabbit monoclonal 56G8 antibody (Cell Signaling, catalog n° 9258).

After rinsing the membrane in PBS, the secondary antibodies used were IRDye 800-conjugated goat anti-rabbit IgG (Rockland, catalog n°611-132-122), IRDye 800-conjugated goat anti-mouse IgG (Rockland, catalog n°610-132-121), Alexa Fluor 680-conjugated goat anti-rabbit IgG (Molecular Probes, catalog n°A21109) or Alexa Fluor 680-conjugated goat anti-mouse IgG (Molecular Probes, catalog n°A21058) all diluted 1:5000 in blocking solution (TBS-T with milk). For phospho-PERK, anti-rabbit HRP (Jackson Immunoresearch Laboratories, catalog n° 211-035-109) diluted 1:10000 was used. Membranes were washed in TBS-T after incubation with the first and the second antibodies. Visualization was performed using the Odyssey infrared imaging device and software (Licor, Hamburg, Germany).

2.4. Apoptosis

Apoptosis of MIN6 cells was determined by scoring the number of cells displaying pycnotic and/or fragmented nucleus after fixation in PBS, 2% paraformaldehyde and staining with Hoechst 33342 (floating apoptotic cells were included).

2.5. Bax immunoprecipitation

MIN6 cells were lysed in 500 µl CHAPS buffer [1% CHAPS, 10 mM Hepes pH 7,4, 150 mM NaCl]. The lysates (700 µg) were incubated with 1.5 µl of the 6A7 Bax monoclonal antibody recognizing the active form of Bax (Santa Cruz, catalog n°23959) overnight with gentle rotation. The next day, 10 µl of protein G-

ACCEPTED MANUSCRIPT

sepharose beads were added and the incubation resumed for 2 additional hours. The beads were then washed three times with CHAPS buffer, mixed with loading buffer, boiled and loaded on a gel for subsequent Western blot analysis.

2.6. Immunocytochemistry

Cells on coverslips were washed with PBS, fixed with PBS, 2% paraformaldehyde and stained with 2.5 mg/ml Hoechst 33342. Following washing with PBS, the cells were permeabilized with 0.2 % (v:v) Triton X-100 in PBS for 10 minutes. The cells were then incubated in 10% FCS-containing DMEM for at least 20 minutes and incubated one hour with various primary antibodies: the 1E9 monoclonal antibody (called I14 in Lefrancois and Lyles, 1982) recognizing the correctly folded form of vesicular stomatatis virus glycoprotein (VSVG) (diluted 1:200), the 17-2-21-4 monoclonal antibody recognizing the VSVG protein exoplasmic domain (diluted 1:100), and the mouse IgG1κmonoclonal antibody specific for GM130 (Golgi

matrix protein of 130 kDa) (BD Biosciences, catalog n°610822) (diluted 1:500). After a washing step in PBS, the cells were incubated with a Cy3-conjugated donkey anti-mouse IgG (Jackson Immunoresearch, catalog n°715-165-151) diluted 1:200 in 10% FCS-containing DMEM one hour at room temperature. Finally, 6 washes in PBS over a 6 hour period were performed before mounting the coverslips in mounting medium for fluorescence [either Vectashield from Vector laboratories, catalog n° H1000 or 0.1 g/ml Mowiol, 0.22% (v/v) glycerol, Tris 0.1 M pH 8.5, 0.1% diazobicyclo-octane]. Images were acquired using a Nikon Eclipse 90i microscope.

2.7. RNA extraction

RNA was extracted by lysing cells, which were initially seeded at a density of 0.5 million cells per well in six-well plates and cultured 2 days, with 500 µl TRI buffer (1.7 M guanidinium thiocyanate, 0.1 M sodium citrate, 0.25% sarcosyl, 0.05 M β-mercaptoethanol, 0.1 M sodium acetate). Chloroform was then added (200 µl) and the lysates were vortexed. The samples were spun 15 min at maximum speed in an Eppendorf centrifuge and the aqueous phase transferred into a new tube containing 500 µl of isopropanol. The tubes were vortexed and kept at -20°C overnight. After spinning 20 min at maximum speed, isopropanol was aspirated and the pellets were washed with 800 µl ethanol 70% before being dried 5-10

ACCEPTED MANUSCRIPT

min at 50°C. Pellets were resuspended in 50 µl of high-quality water and RNA was quantitated using a NanoDrop device (NanoDrop 2000c, Thermo Fisher Scientific). Alternatively RNA was extracted using the High pure RNA Isolation Kit from Roche (catalog n°11828665001).

2.8. Reverse transcription

For reverse transcription, 0.5 µg of RNA was mixed with 500 ng of random hexamers (ordered from Microsynth, Balgach, Switzerland) in a total volume of water of 11 µl, incubated 3 minutes at 70°C and then placed on ice for 3 minutes. To this, 14 µl of a mix was added that contained 5 µl of a 10 mM dNTPs solution (Promega catalog n° U120D- U123D), 0.5 µl of RNasin (Promega, catalog n°N211A), 5 µl of buffer 5x, 2 µl DTT, 0.5 µl Superscript reverse transcriptase and 1 µl of water, everything provided in the Superscript II reverse Transcriptase Kit (Invitrogen, catalog n°18064-014). After incubation at 39°C for 1 hour followed by 15 minutes at 70°C, the cDNA was diluted 1:3. Alternatively, reverse transcription was performed using the Transcriptor High Fidelity cDNA Synthesis Kit from Roche (catalog n°05 091 284 001).

2.9. Quantitative PCR

qPCR assays were carried out on a real-time PCR detection system (iQ5; Bio-Rad) using iQ SYBR Green Supermix (Bio-Rad, catalog n°170-8880) using 100 nM primers, 1 µl of template (reverse transcription samples [see section above] diluted 1:3 in water) per 20 µl of PCR and an annealing temperature of 59°C. Melting curve analyses were performed on all PCRs to rule out non-specific amplification. Reactions were carried out in triplicates. The following primers were used: RPLP0 sense (5'-ACCTCCTTCTTCCAGGCTTT-3') and antisense (5'-AAAGACTGGAGACAAGGTGG-3'), 18S sense (5'-GCAATTATTCCCCATGAACG-3') and antisense (5'-GGCCTCACTAAACCATCCAA-3'), CHOP sense (5'-TTCACTACTCTTGACCCTGCGTC-3') and antisense (5'-CACTGACCACTCTGTTTCCGTTTC-3'), spliced XBP1 sense (GAGTCCGCAGCAGGTG) and antisense (GTGTCAGAGTCCATGGGA), total XBP1 sense (AAGAACACGCTTGGGAATGG) and antisense (ACTCCCCTTGGCCTCCAC).

2.10. XBP1 mRNA splicing

ACCEPTED MANUSCRIPT

Touchdown PCRs were performed using XBP1 sense (5'-AAACAGAGTAGCAGCGCAGACTGC-3') and antisense (5'-GGATCTCTAAAACTAGAGGCTTGGTG-3') primers and the Taq polymerase from Promega (catalog n°M830B). PCR products were loaded on a 4% agarose gel and run for about 6 hours to discriminate the 26 nucleotides difference between the expected spliced and unspliced forms. Two bands were generated in addition to the lower band that corresponds to the spliced XBP1 mRNA (see Figure 2, panel A). To determine which one of the two upper bands was non-specifically amplified, the PCR products were digested with PstI and run on a 4% gel for 1 hour. The PCR fragment amplified from the unspliced XBP1 mRNA contains a PstI restriction site more or less in its middle. When cleaved, this fragment should therefore disappear from the region where ~600 bp fragments migrate to. The band labeled with # in Figure 1A was not cleaved by PstI and is therefore an unspecific fragment.

2.11. Lentivirus

HEK293T cells were co-transfected using the calcium phosphate DNA precipitation method (Jordan et al., 1996) with 10 µg of the lentiviral vector containing the shRNA or the cDNA of interest, 2.5 µg of the envelope protein–coding plasmid (pMD.G), and 7.5 µg of the packaging construct (pCMVDR8.91). Two days later, the virus-containing medium was harvested. Infection of the cells was performed as follows. Hexadimethrine bromide (Polybrene; Sigma, catalog n°52495) was added to cells cultured in six-well plates to a final concentration of 5 µg/ml followed by the addition of the lentiviruses. The plates were placed 24 hours at 37°C in a 5% CO_2 humidified atmosphere. The medium was then replaced with fresh medium, and the cells were further cultured for an additional 48-hour period.

2.12. Folding assay

MIN6 cells were plated on coverlips and infected with 2.5 ml of a VSVG-GFP encoding lentivirus. Two days later, the cells were treated as mentioned in the figure legend. Cells were then fixed and cells on coverslips were labeled by immunocytochemistry.

2.13. Lipoprotein preparation and purification

HDLs were prepared as described earlier (Petremand et al., 2012).

ACCEPTED MANUSCRIPT

2.14. Plasmids

Plasmid tsVSVG-GFP.lti (#730) is a lentiviral expression vector encoding a fusion protein between the temperature sensitive ts045 variant of vesicular stomatitis virus G protein (Presley et al., 1997) and GFP (Petremand et al., 2012).

2.15. Electron microscopy

MIN6 cells were plated in poly-L-lysine (0.01%, Sigma, catalog n°P4832)-coated glass slides (LabTek Chamber Slides, catalog n°177399) at a density of 110'000 cells per slide (area = 1.8 cm2), cultured for 3 days, and finally treated as indicated in the figures. Cells were then fixed 2 hours in 2.5% glutaraldehyde (Electron Microscopy Sciences, catalog n°16220) dissolved in 0.1 M phosphate buffer (PB), pH 7.4. After 3 washes in PB, MIN6 cells were post-fixed for 1 hour in 1% osmium tetroxide (Electron Microscopy Sciences, catalog n°19150) in PB, and then stained with ethanol 70% containing 1% uranyl acetate (Sigma, catalog n°73943) for 20 minutes. MIN6 cells were dehydrated in graded alcohol series and embedded in Epon (Electron Microscopy Sciences, catalog n°13940). Ultrathin sections (with silver to gray interference) were cut with a diamond knife (Diatome), mounted on Formvar-coated single slot grids and then counterstained with 3% uranyl acetate for 10 minutes and then with lead citrate (0.2%, Sigma, catalog n°15326) for 10 minutes. Sections were visualized using a Philips CM100 transmission electron microscope.

2.16. Quantification of the ER thickness

To evaluate the effect of the treatments on the ER integrity, the ER thickness was evaluated following each treatment. To do so, for each cell, the averaged thickness of ER per cell (i.e. the mean of the thickness of 20 ER figures per cell) was calculated. For each ER figure, the relative thickness was defined as the ratio between the area of the ER element and its Feret's diameter. The Feret's diameter, also called the caliper length, is the longest distance between any two points along a region of interest boundary. The area and the Feret's diameter were measured using the Image J software. The results shown for each condition represent the mean of 50 cells.

ACCEPTED MANUSCRIPT

2.17. Data presentation and statistics

The data in the figures are presented as the mean ± 95% confidence intervals. Statistical significance in Figures 4-7 was assessed by one-way ANOVA with post-hoc Bonferroni-Dunn testing. In Figure 3, the data were not following a normal distribution and were thus analyzed using a Kruskal-Wallis one-way ANOVA and unpaired Wilcoxon tests with Bonferroni correction.

ACCEPTED MANUSCRIPT

3. Results

3.1. HDLs protect Min6 cells against tunicamycin-induced apoptosis

HDLs have been shown to protect pancreatic beta cells against death induced by various ER stressors (Petremand et al., 2009; Petremand et al., 2012; Rutti et al., 2009) including TM, a N-glycosylation inhibitor [Figure 1A and (Petremand et al., 2009)]. To determine if the protection conferred by HDLs on TM-treated beta cells was associated with an inhibition of the mitochondrial apoptotic pathway, the Min6 mouse beta cell line was incubated with TM in the presence or in the absence of HDLs. The extent of caspase-3 activation and Bax activation was then assessed. Figure 1B shows that HDLs inhibited TM-induced apoptosis in Min6 cells and that this correlated with a reduction in the cleavage of full-length caspase-3 into the active form of the protease. Moreover, HDLs hampered TM-induced Bax activation (Figure 1C). These results indicate that HDLs efficiently prevent TM-induced beta cell death most likely by antagonizing the intrinsic mitochondrial apoptotic death pathway.

3.2. HDLs inhibit tunicamycin-induced ER morphological alterations

HDLs allow beta cells to preserve their ER morphology in the presence of ER stressors such as palmitate and TG (Petremand et al., 2012). We therefore wished to determine if the protection conferred by HDLs against TM-induced beta cells death was also associated with the maintenance of a normal ER morphology. A 6 hour-incubation with TM induced a moderate ER ballooning but no obvious alterations of other organelles (Figure 2A). ER ballooning was more extensive when the cells were incubated with TM for 24 hours (Figure 2B) and this was associated with the appearance of DNA condensation typically seen in apoptotic cells (asterisks in Figure 2B). The ballooning stimulated by TM was markedly reduced by HDLs but not fully abolished (Figure 3). As reported earlier, HDLs totally prevented the strong ER ballooning induced by TG (Figure 3). Altogether, these results indicate that HDLs have a broad capacity to preserve ER morphology in the presence of various ER stressors.

ACCEPTED MANUSCRIPT

3.3. HDLs do not prevent tunicamycin-induced ER stress marker increase

In beta cells, the ER stress response induced by TG, cyclopiazonic acid, and palmitate is efficiently inhibited by HDLs (Petremand et al., 2012). Specifically, in response to these agents, HDLs repressed XBP-1 splicing, CHOP and BiP induction, and PERK and JNK activation (Petremand et al., 2012) that are all markers of the unfolded protein response activated following ER stress (Hetz, 2012). It was therefore expected that the ability of HDLs to counteract TM-induced apoptosis in Min6 cells would also result in inhibition of ER stress response induction. This was, surprisingly, not the case: TM-induced XBP-1 splicing was not altered by HDLs (Figure 4A and B). There was a trend of a slight decrease in BiP expression (Figure 4B), PERK activation (Figure 4C), and CHOP induction at the mRNA and protein levels (Figure 4D-E) but this did not reach statistical significance. These results indicate that HDLs can inhibit apoptosis of beta cells subjected to ER stress when several arms of the UPR are activated.

3.4. HDLs do not restore ER protein folding and trafficking impaired by tunicamycin

It was recently demonstrated that, in the presence of ER stressors, HDLs maintain the ER protein folding capacity of beta cells and allow protein trafficking from the ER to the plasma membrane via the Golgi (Petremand et al., 2012). To assess if HDLs have the same beneficial effect on the ER in TM-stimulated beta cells, we employed a fusion protein between the green fluorescence protein (GFP) and a temperature-sensitive mutant of the vesicular stomatitis virus G (VSVG) protein (Presley et al., 1997). This fusion protein traffics from the ER to the plasma membrane via the Golgi apparatus at the permissive temperature of 32°C. At 40°C degrees however, the fusion protein is misfolded and accumulates in the ER. Switching the temperature back to 32°C allows proper refolding of the VSVG-GFP fusion protein and resuming of the protein transport to the cell surface (Petremand et al., 2012; Presley et al., 1997). MIN6 cells were infected with lentiviruses encoding the VSVG fusion protein. They were then treated with TM in the presence or in the absence of HDLs and incubated at 40°C for 5 hours. The block at 40°C, which impairs folding of the VSVG-GFP mutant, led to its accumulation in the ER (Figure 5, upper row). Cells

ACCEPTED MANUSCRIPT

were then incubated for 1 hour at 32°C to allow VSVG-GFP folding and trafficking to the membrane. In the control condition, after 1 hour at 32°C, VSV-G was correctly folded and was localized at the plasma membrane (Figure 5, second row from the top). However, in the presence of TM, VSV-G did not traffic to the membrane and the percentage of cells with folded VSV-G was strongly reduced compared to the control (Figure 5, third row from the top). HDLs were unable to reverse these defects (Figure 5, lower row), which mirrors their inability to prevent ER stress marker induction by TM (see Figure 4).

3.4. Effects of HDL on ER stressor-induced Akt and JNK modulation

In Min6 cells, TM and TG have been shown, on one hand, to reduce basal activation of Akt and, on the other hand, to stimulate the JNK MAPK pathway (Srinivasan et al., 2005). These effects could be mitigated by insulin-like growth factor 1 (IGF1) (Srinivasan et al., 2005). HDLs may have a similar effect, which could partly explain how they protect cells against TM-induced apoptosis despite their inability to restore ER functionality. We therefore tested the potential Akt and JNK modulatory role of HDLs in the presence of various ER stressors, including TM. Figure 6A shows that HDLs efficiently inhibited apoptosis of Min6 cells induced by TG, TM, inflammatory cytokines, and palmitate, compounds that have all shown to provoke ER stress (Kharroubi et al., 2004; Petremand et al., 2009). As reported (Srinivasan et al., 2005), TG and TM decreased basal Akt activation (Figure 6B). HDLs significantly blunted this decrease. However, this dampening effect was rather weak when Min6 cells were treated with TG. Inflammatory cytokines and palmitate induced a marked activation of Akt that was not modulated by HDLs. There is therefore no clear correlation between Akt stimulation levels and beta cell protection. Possibly, Akt contributes to beta cell protection but by itself can apparently not induce efficient beta cell survival.

JNKs were activated by TG and HDLs had a tendency to reduce this response but this did not reach statistical significance (Figure 6C). Inflammatory cytokines also stimulated the JNK MAPK pathway. However, this was not modulated by HDLs. TM and palmitate, in the conditions used here, did not stimulate the JNKs. These results indicate that inhibition of the JNK pathway is not a mechanism used by HDLs to protect beta cells.

ACCEPTED MANUSCRIPT

3.5. HDLs are protecting Min6 cells at submicromolar concentrations

When addressing HDL functions in pancreatic cells, one needs to consider the concentrations that may be found outside the vascular system. Intuitively, it could be expected that HDL concentrations are low in the extravascular space. However, the available data indicate that the vascular and extra vascular HDL concentrations are not very much different. For example, the HDL concentrations in the lymph and in synovial fluid were measured to be 0.4 +/- 0.1 mM and 0.7 +/- 0.1 mM, respectively (Busso et al., 2001; Nanjee et al., 2001) which is not far away from the blood HDL concentrations (1-1.5 mM). This suggests an active transport of HDLs through the vasculature, the mechanism of which starts to be unraveled (Cavelier et al., 2012; Ohnsorg et al., 2011; Rohrer et al., 2009). To assess the physiological relevance of our results, we determined if HDLs in the concentration range found in extravascular tissues (0.4 to 0.7 mM) can protect MIN6 cells. Figure 6 shows that HDLs can inhibit TM- and TG-induced MIN6 apoptosis at doses as low as 0.25 mM. This suggests that extravascular HDL levels can protect beta cells against ER stressors.

ACCEPTED MANUSCRIPT

4. Discussion

The present work indicates that HDLs can protect pancreatic beta cells against TM-induced apoptosis despite the continuous activation of UPR pathways and impairment of the ER functionality (protein folding and trafficking). This contrasts with earlier data indicating that HDLs block TG-induced beta cell death by maintaining proper functioning of the ER (Petremand et al., 2012). HDLs have therefore at least two ways of protecting beta cells. They can prevent ER dysfunctions and the resulting stress response induced by drugs such as TG and pro-diabetogenic lipids such as palmitate. If this first line of defense cannot be established, such as when TM is used, HDLs can still protect beta cells downstream of ER stress response activation (Figure 8).

It could be argued that HDLs can inhibit an ER stress response only if this stress response is not too strong. However, the activation of the ER stress pathway by TG and TM at the concentration used here (0.5 µM and 2 µg/ml, respectively) was found to be comparable when BiP expression is considered [see Figure 7 in (Petremand et al., 2009). This can also be seen by comparing Figure 4 of the present work with Figure 2 of reference (Petremand et al., 2012) that were both derived from the same set of data. For other stress markers like the induction of ATF4 [see Figure 7 in (Petremand et al., 2009)] or the induction of CHOP mRNA and protein levels [compare Figure 4 of the present work with Figure 2 of reference (Petremand et al., 2012)], 2 µg/ml of TM induced a weaker response compared to 0.5 µM TG. We also note that TG-induced ER ballooning was much more pronounced than when TM was employed (Figure 3). The extent of ER stress and UPR activation by TM does not therefore appear to be stronger than the one induced by TG, at least with the doses used in the present study, indicating that the ability of HDLs to inhibit UPR induction depends more on the nature of the ER stressors rather than the extent of the stress itself.

It has to be pointed out however that the data shown in Figure 4 suggest that HDLs may lead to a partial, albeit non-significant, decrease in the induction of some ER stress markers, CHOP mRNA and protein levels in particular, but as detailed in the previous paragraph, HDLs were clearly less efficient in diminishing the possibly weaker UPR activated by TM compared to the UPR induced by TG.

ACCEPTED MANUSCRIPT

There are precedents of beta cell protection against ER stressor-induced death in spite of continuous activation of the UPR. It was indeed reported that IGF-1 protects, or at least delays, TM-induced MIN6 cell apoptosis assessed by PARP cleavage even though TM-mediated CHOP induction was unaffected (Srinivasan et al., 2005).

Decreased Akt stimulation often compromises beta cell survival (Li et al., 2005; Natalicchio et al., 2010; Storling et al., 2005; Yano et al., 2007) but this is not always the case. In mice expressing the myristoylated constitutive form of Akt (myr-Akt) specifically in insulin-producing cells, basal apoptosis in beta cells is increased by at least ten fold while streptozotocin-induced beta cell apoptosis is inhibited by ~80% (Tuttle et al., 2001). The survival response after Akt activation in resting beta cells and stressed beta cells diverges therefore. Transfection of the INS1 insulinoma cell line with myr-Akt-encoding plasmids induces their death in an NFkB-dependent manner (Bulat et al., 2011) but infecting the same cell line with myr-Akt-encoding adenoviruses protects them against a cocktail of inflammatory cytokines (Li et al., 2005). Possibly, theses opposite results originate from different Akt expression levels achieved by either transfection or infection. The role of Akt in the control of beta cell survival is therefore highly context-dependent, which presumably is at the basis of the apparent conflicting observations that Akt, depending on the experimental conditions, either promotes or inhibits apoptosis in beta cells. In the present study, Akt was activated by palmitate and inflammatory cytokines but this did not result in beta cell protection. An earlier study reported a palmitate-induced Akt activation in INS1 cells and this activation led to reduced viability and/or proliferation (Higa et al., 2006). Inflammatory cytokines (IL1β, IFNγ, with or without TNFα), on the other hand, are generally reported to induce decreased Akt activation (Li et al., 2005; Natalicchio et al., 2010) but the beta cell death induced by these cytokines may only partially results from Akt down-regulation (Li et al., 2005). The reason why an increased Akt activation following stimulation of Min6 cells was observed in the present study and not in others is unclear but may be related to the extent of the cellular stress experienced by the beta cells in the various experimental systems. The extent of cellular stress can be evaluated by the p120 RasGAP protein, a sensor of caspase-3 activity (Khalil et al., 2012; Khalil et al., 2013). In response to weak stresses, caspase-3 activity raises in cells, but to minimal extent, and this results in the partial cleavage of RasGAP into an N-terminal fragment, called fragment N, that can protect cells by activating Akt (Yang et al., 2004). Fragment N can protect beta cells against a variety of

ACCEPTED MANUSCRIPT

pro-diabetogenic insults both in vitro and in vivo (Bulat et al., 2011; Yang et al., 2009; Yang et al., 2005). If the stress becomes too intense so as to become pro-apoptotic, fragment N is further cleaved by the now higher caspase-3 activity, abrogating its capacity to stimulate Akt (Yang et al., 2005). The sequential cleavage of RasGAP regulated by increasing caspase-3 activation can therefore determine whether a stressed cell survives or not (Khalil et al., 2013). However, there are stress-inducing factors that, despite allowing the formation of fragment N, cannot efficiently prevent further caspase-3 activation and apoptosis (Khalil et al., 2012). In such cases, Akt can nevertheless be activated but this is not counteracting apoptosis and may just represent a futile attempt of the cell to protect itself. Possibly, Akt activation by cytokines corresponds to a similar phenomenon. This could be tested by determining if inflammatory cytokine-induced Akt activation is prevented by caspase inhibitors.

Inflammatory cytokines are well-known for their ability to activate the NFkB factor in pancreatic beta cells (Donath et al., 2008). Even though NFkB is usually considered a downstream effector of Akt (Salminen and Kaarniranta, 2010), it has been suggested that Akt in beta cells could be activated following NFkB stimulation in some situations (Storling et al., 2011). Whether cytokines have the potential to stimulate Akt via NFkB is therefore a possibility that could be experimentally addressed in the future.

What prevents HDLs from inhibiting the induction of the UPR in response to stresses such as TM? Even if HDLs have an initial capacity to maintain the functionality of the ER in TM-treated cells, the inhibition of protein glycosylation by TM would anyway not permit proper protein trafficking and this would ultimately results in increased protein load and misfolding in the ER leading to augmented ER stress and ER malfunction. In contrast, TG does not directly affect ER-resident proteins but rather the biophysical properties of the ER lumen by decreasing the ER calcium concentration (Sambrook, 1990). In this situation, HDL-mediated maintenance of ER functionality allows protein to fold and traffic properly hence reducing ER stress (Petremand et al., 2012). Palmitate also provokes a drop in ER calcium concentration in several cell types including pancreatic beta cells (Gwiazda et al., 2009; Wei et al., 2009). In this case too, HDLs allow proper protein trafficking and correct protein folding in the ER and this alleviates the ER stress that palmitate would otherwise stimulate (Petremand et al., 2012). Therefore, HDLs may not be able to prevent ER stress induced by drugs and conditions that directly alter proteins in a way that

ACCEPTED MANUSCRIPT

prevents them from folding and trafficking correctly. In contrast, HDLs can inhibit ER stress by maintaining the ER functionality in the presence of drugs and conditions that alter the bio-physical properties of the ER, but not directly the ER proteins. This model is consistent with the observation that over-expression of wild-type insulin in beta cells leads to an ER stress that can be inhibited by HDLs, while the ER stress induced by over-expression of the C96Y insulin mutant that does not fold properly cannot (Petremand et al., 2012).

Interestingly, HDLs can prevent ER morphology alterations (i.e. ER ballooning) induced by both TG and TM. Since HDLs inhibit induction of the UPR by TG but not by TM, one can conclude that there is dissociation between ER ballooning and UPR. To our knowledge, the pathway leading to ER swelling or ballooning is not characterized yet. Our results indicate nevertheless that this uncharacterized ER stress-induced pathway involve proteins or lipids that can be targeted by HDLs.

The nature of the signaling pathways activated by HDLs that on one hand favor ER functions (e.g. in the presence of TG) and on the other hand protects beta cells despite the presence of an ER stress (e.g. in the presence of TM) currently remain a mystery. Identification of these pathways is of clear clinical importance as this is a pre-requisite for the development of drugs that stimulate or mimic the anti-diabetic effects of HDLs to lower the risk, for example in overweight patients, of developing type 2 diabetes.

Funding

C.W. is supported by grants from the Swiss National Science Foundation (no. 31003A_141242/1) and the Swiss Cancer League (no. KFS-02543-02-2010).

Acknowledgements

The authors thank Jean Daraspe (University of Lausanne, Switzerland) for technical assistance and the Electron Microscopy Facility at the University of Lausanne for the use of electron microscopes. We thank the laboratory of Romano Regazzi (University of Lausanne, Switzerland) for providing inflammatory cytokines.

ACCEPTED MANUSCRIPT

Reference List

1. Abderrahmani, A., Niederhauser, G., Favre, D., Abdelli, S., Ferdaoussi, M., Yang, J.Y., Regazzi, R., Widmann, C., Waeber, G., 2007. Human high-density lipoprotein particles prevent activation of the JNK pathway induced by human oxidised low-density lipoprotein particles in pancreatic β cells. Diabetologia 50, 1304-1314.

2. Al-Jarallah, A., Trigatti, B.L., 2010. A role for the scavenger receptor, class B type I in high density lipoprotein dependent activation of cellular signaling pathways. Biochimica et Biophysica Acta 1801, 1239-1248.

3. Bulat, N., Jaccard, E., Peltzer, N., Khalil, H., Yang, J.Y., Dubuis, G., Widmann, C., 2011. RasGAP-derived fragment N increases the resistance of beta cells towards apoptosis in NOD mice and delays the progression from mild to overt diabetes. PLoS.ONE. 6, e22609.

4. Busso, N., Dudler, J., Salvi, R., Peclat, V., Lenain, V., Marcovina, S., Darioli, R., Nicod, P., So, A.K., Mooser, V., 2001. Plasma apolipoprotein(a) co-deposits with fibrin in inflammatory arthritic joints. American Journal of Pathology 159, 1445-1453.

5. Cavelier, C., Ohnsorg, P.M., Rohrer, L., von Eckardstein, A., 2012. The beta-chain of cell surface F(0)F(1) ATPase modulates apoA-I and HDL transcytosis through aortic endothelial cells. Arteriosclerosis, Thrombosis, and Vascular Biology 32, 131-139.

6. Cnop, M., Hannaert, J.C., Grupping, A.Y., Pipeleers, D.G., 2002. Low density lipoprotein can cause death of islet beta-cells by its cellular uptake and oxidative modification. Endocrinology 143, 3449-3453.

7. Donath, M.Y., Storling, J., Berchtold, L.A., Billestrup, N., Mandrup-Poulsen, T., 2008. Cytokines and beta-cell biology: from concept to clinical translation. Endocrine Reviews 29, 334-350.

8. Drew, B.G., Duffy, S.J., Formosa, M.F., Natoli, A.K., Henstridge, D.C., Penfold, S.A., Thomas, W.G., Mukhamedova, N., de Court, Forbes, J.M., Yap, F.Y., Kaye, D.M., van Hall, G., Febbraio, M.A., Kemp, B.E., Sviridov, D., Steinberg, G.R., Kingwell, B.A., 2009. High-density lipoprotein modulates glucose metabolism in patients with type 2 diabetes mellitus. Circulation 119, 2103-2111.

9. Eizirik, D.L., Cardozo, A.K., Cnop, M., 2008. The role for endoplasmic reticulum stress in diabetes mellitus. Endocrine Reviews 29, 42-61.

10. Eizirik, D.L., Cnop, M., 2010. ER stress in pancreatic beta cells: the thin red line between adaptation and failure. Science Signaling 3, e7.

11. Fryirs, M.A., Barter, P.J., Appavoo, M., Tuch, B.E., Tabet, F., Heather, A.K., Rye, K.A., 2010. Effects of high-density lipoproteins on pancreatic beta-cell insulin secretion. Arteriosclerosis, Thrombosis, and Vascular Biology 30, 1642-1648.

ACCEPTED MANUSCRIPT

12. Gwiazda, K.S., Yang, T.L., Lin, Y., Johnson, J.D., 2009. Effects of palmitate on ER and cytosolic Ca^{2+} homeostasis in βcells. American Journal of Physiology - Endocrinology and Metabolism 296, E690-E701.

13. Hetz, C., 2012. The unfolded protein response: controlling cell fate decisions under ER stress and beyond. Nature Reviews Molecular Cell Biology 13, 89-102.

14. Higa, M., Shimabukuro, M., Shimajiri, Y., Takasu, N., Shinjyo, T., Inaba, T., 2006. Protein kinase B/Akt signalling is required for palmitate-induced beta-cell lipotoxicity. Diabetes Obes.Metab. 8, 228-233.

15. Jordan, M., Schallhorn, A., Wurm, F.M., 1996. Transfecting mammalian cells: optimization of critical parameters affecting calcium-phosphate precipitate formation. Nucleic Acids Research 24, 596-601.

16. Khalil, H., Bertrand, M.J., Vandenabeele, P., Widmann, C., 2013. Caspase-3 and RasGAP: a stress-sensing survival/demise switch. Trends in Cell Biology in press.

17. Khalil, H., Peltzer, N., Walicki, J., Yang, J.Y., Dubuis, G., Gardiol, N., Held, W., Bigliardi, P., Marsland, B., Liaudet, L., Widmann, C., 2012. Caspase-3 protects stressed organs against cell death. Mol.Cell Biol. 32, 4523-4533.

18. Khalil, H., Rosenblatt, N., Liaudet, L., Widmann, C., 2012. The role of endogenous and exogenous RasGAP-derived fragment N in protecting cardiomyocytes from peroxynitrite-induced apoptosis. Free.Radic.Biol.Med. 53, 926-935.

19. Kharroubi, I., Ladriere, L., Cardozo, A.K., Dogusan, Z., Cnop, M., Eizirik, D.L., 2004. Free fatty acids and cytokines induce pancreatic beta-cell apoptosis by different mechanisms: role of nuclear factor-κB and endoplasmic reticulum stress. Endocrinology 145, 5087-5096.

20. Kimura, T., Tomura, H., Sato, K., Ito, M., Matsuoka, I., Im, D.S., Kuwabara, A., Mogi, C., Itoh, H., Kurose, H., Murakami, M., Okajima, F., 2010. Mechanism and role of high density lipoprotein-induced activation of AMP-activated protein kinase in endothelial cells. Journal of Biological Chemistry 285, 4387-4397.

21. Lefrancois, L., Lyles, D.S., 1982. The interaction of antibody with the major surface glycoprotein of vesicular stomatitis virus. I. Analysis of neutralizing epitopes with monoclonal antibodies. Virology 121, 157-167.

22. Li, L., El-Kholy, W., Rhodes, C.J., Brubaker, P.L., 2005. Glucagon-like peptide-1 protects beta cells from cytokine-induced apoptosis and necrosis: role of protein kinase B. Diabetologia 48, 1339-1349.

23. Nanjee, M.N., Cooke, C.J., Wong, J.S., Hamilton, R.L., Olszewski, W.L., Miller, N.E., 2001. Composition and ultrastructure of size subclasses of normal human peripheral lymph lipoproteins: quantification of cholesterol uptake by HDL in tissue fluids. J.Lipid.Res. 42, 639-648.

24. Natalicchio, A., De, S.F., Orlando, M.R., Melchiorre, M., Leonardini, A., Cignarelli, A., Labarbuta, R., Marchetti, P., Perrini, S., Laviola, L., Giorgino, F., 2010. Exendin-4 prevents c-Jun N-terminal

ACCEPTED MANUSCRIPT

protein kinase activation by tumor necrosis factor-alpha (TNFα) and inhibits TNFα-induced apoptosis in insulin-secreting cells. Endocrinology 151, 2019-2029.

25. Nofer, J.R., Levkau, B., Wolinska, I., Junker, R., Fobker, M., von Eckardstein, A., Seedorf, U., Assmann, G., 2001. Suppression of endothelial cell apoptosis by high density lipoproteins (HDL) and HDL-associated lysosphingolipids. Journal of Biological Chemistry 276, 34480-34485.

26. Nofer, J.R., van der, G.M., Tolle, M., Wolinska, I., von Wnuck, L.K., Baba, H.A., Tietge, U.J., Godecke, A., Ishii, I., Kleuser, B., Schafers, M., Fobker, M., Zidek, W., Assmann, G., Chun, J., Levkau, B., 2004. HDL induces NO-dependent vasorelaxation via the lysophospholipid receptor S1P3. Journal of Clinical Investigation 113, 569-581.

27. Ohnsorg, P.M., Rohrer, L., Perisa, D., Kateifides, A., Chroni, A., Kardassis, D., Zannis, V.I., von Eckardstein, A., 2011. Carboxyl terminus of apolipoprotein A-I (ApoA-I) is necessary for the transport of lipid-free ApoA-I but not prelipidated ApoA-I particles through aortic endothelial cells. Journal of Biological Chemistry 286, 7744-7754.

28. Petremand, J., Bulat, N., Butty, A.C., Poussin, C., Rutti, S., Au, K., Ghosh, S., Mooser, V., Thorens, B., Yang, J.Y., Widmann, C., Waeber, G., 2009. Involvement of 4E-BP1 in the protection induced by HDLs on pancreatic beta cells. Molecular Endocrinology 23, 1572-1586.

29. Petremand, J., Puyal, J., Chatton, J.Y., Duprez, J., Allagnat, F., Frias, M., James, R.W., Waeber, G., Jonas, J.C., Widmann, C., 2012. HDLs protect pancreatic beta-cells against ER stress by restoring protein folding and trafficking. Diabetes 61, 1100-1111.

30. Presley, J.F., Cole, N.B., Schroer, T.A., Hirschberg, K., Zaal, K.J., Lippincott-Schwartz, J., 1997. ER-to-Golgi transport visualized in living cells. Nature 389, 81-85.

31. Rohrer, L., Hersberger, M., von Eckardstein, A., 2004. High density lipoproteins in the intersection of diabetes mellitus, inflammation and cardiovascular disease. Current Opinion in Lipidology 15, 269-278.

32. Rohrer, L., Ohnsorg, P.M., Lehner, M., Landolt, F., Rinninger, F., von Eckardstein, A., 2009. High-density lipoprotein transport through aortic endothelial cells involves scavenger receptor BI and ATP-binding cassette transporter G1. Circ.Res. 104, 1142-1150.

33. Rutti, S., Ehses, J.A., Sibler, R.A., Prazak, R., Rohrer, L., Georgopoulos, S., Meier, D.T., Niclauss, N., Berney, T., Donath, M.Y., von Eckardstein, A., 2009. Low and high-density lipoproteins modulate function, apoptosis and proliferation of primary human and murine pancreatic beta cells. Endocrinology 150, 4521-4530.

34. Salminen, A., Kaarniranta, K., 2010. Insulin/IGF-1 paradox of aging: regulation via AKT/IKK/NF-kappaB signaling. Cell Signal. 22, 573-577.

35. Sambrook, J.F., 1990. The involvement of calcium in transport of secretory proteins from the endoplasmic reticulum. Cell 61, 197-199.

36. Srinivasan, S., Ohsugi, M., Liu, Z., Fatrai, S., Bernal-Mizrachi, E., Permutt, M.A., 2005. Endoplasmic reticulum stress-induced apoptosis is partly mediated by reduced insulin signaling

ACCEPTED MANUSCRIPT

through phosphatidylinositol 3-kinase/Akt and increased glycogen synthase kinase-3βin mouse insulinoma cells. Diabetes 54, 968-975.

37. Storling, J., Binzer, J., Andersson, A.K., Zullig, R.A., Tonnesen, M., Lehmann, R., Spinas, G.A., Sandler, S., Billestrup, N., Mandrup-Poulsen, T., 2005. Nitric oxide contributes to cytokine-induced apoptosis in pancreatic beta cells via potentiation of JNK activity and inhibition of Akt. Diabetologia 48, 2039-2050.

38. Storling, J., Juntti-Berggren, L., Olivecrona, G., Prause, M.C., Berggren, P.O., Mandrup-Poulsen, T., 2011. Apolipoprotein CIII reduces proinflammatory cytokine-induced apoptosis in rat pancreatic islets via the Akt prosurvival pathway. Endocrinology 152, 3040-3048.

39. Tuttle, R.L., Gill, N.S., Pugh, W., Lee, J.P., Koeberlein, B., Furth, E.E., Polonsky, K.S., Naji, A., Birnbaum, M.J., 2001. Regulation of pancreatic βcell growth and survival by the serine/threonine protein kinase Akt1/PKBα Nat.Med. 7, 1133-1137.

40. von Eckardstein, A., Schulte, H., Assmann, G., 2000. Risk for diabetes mellitus in middle-aged Caucasian male participants of the PROCAM study: implications for the definition of impaired fasting glucose by the American Diabetes Association. Journal of Clinical Endocrinology & Metabolism 85, 3101-3108.

41. von Eckardstein, A., Sibler, R.A., 2011. Possible contributions of lipoproteins and cholesterol to the pathogenesis of diabetes mellitus type 2. Current Opinion in Lipidology 22, 26-32.

42. Wei, Y., Wang, D., Gentile, C.L., Pagliassotti, M.J., 2009. Reduced endoplasmic reticulum luminal calcium links saturated fatty acid-mediated endoplasmic reticulum stress and cell death in liver cells. Molecular and Cellular Biochemistry 331, 31-40.

43. Yang, J.Y., Walicki, J., Jaccard, E., Dubuis, G., Bulat, N., Hornung, J.P., Thorens, B., Widmann, C., 2009. Expression of the NH_2-terminal fragment of RasGAP in pancreatic βcells increases their resistance to stresses and protects mice from diabetes. Diabetes 58, 2596-2606.

44. Yang, J.-Y., Michod, D., Walicki, J., Murphy, B.M., Kasibhatla, S., Martin, S., Widmann, C., 2004. Partial cleavage of RasGAP by caspases is required for cell survival in mild stress conditions. Mol.Cell Biol. 24, 10425-10436.

45. Yang, J.-Y., Walicki, J., Abderrahmani, A., Cornu, M., Waeber, G., Thorens, B., Widmann, C., 2005. Expression of an uncleavable N-terminal RasGAP fragment in insulin-secreting cells increases their resistance toward apoptotic stimuli without affecting their glucose-induced insulin secretion. Journal of Biological Chemistry 280, 32835-32842.

46. Yang, J.-Y., Walicki, J., Michod, D., Dubuis, G., Widmann, C., 2005. Impaired Akt activity down-modulation, caspase-3 activation, and apoptosis in cells expressing a caspase-resistant mutant of RasGAP at position 157. Molecular Biology of the Cell 16, 3511-3520.

47. Yano, T., Liu, Z., Donovan, J., Thomas, M.K., Habener, J.F., 2007. Stromal cell derived factor-1 (SDF-1)/CXCL12 attenuates diabetes in mice and promotes pancreatic beta-cell survival by activation of the prosurvival kinase Akt. Diabetes 56, 2946-2957.

ACCEPTED MANUSCRIPT

Figure legends

Figure 1: HDLs protect beta cells against TM-induced apoptosis

A: MIN6 cells were treated with 2 µg/ml TM for 24 hours or left untreated (C) in the presence or in the absence of 1 mM HDLs and apoptosis was assessed by scoring pycnotic nucleus. Results correspond to the mean ± 95% CI of 6 independent experiments. Asterisks denote statistically significant difference between the indicated conditions as assessed by paired t-test with Bonferroni corrections. B: Alternatively, protein extracts were prepared and the active form of Bax was immunoprecipitated. Western blot against Bax was then performed. #, unspecific band. This experiment was repeated twice and yielded identical results.

Figure 2: HDL effect on TM-induced ER morphology alterations

Representative electron micrographs showing MIN6 cells (low magnification) and ER morphology (high magnification) following treatments with the indicated compounds for 6 hours (panel A) or 24 hours (panel B). Note the ballooning of the ER in TM-treated cells. TM, tunicamycin; N, nucleus; the asterisks indicate DNA condensation.

Figure 3: Comparison of the HDL protective effect against ER morphology alterations induced by tunicamycin and thapsigargin

Representative electron micrographs showing the ER morphology of MIN6 cells stimulated as in Figure 2A (top) and corresponding quantitation of the ER thickness (bottom). ER thickness was evaluated by calculating the area/Feret diameter of individual ER segments of at least 50 cells per condition (see Material and methods). Asterisks over individual bars indicate a statistically significant difference with the control condition. The asterisks over horizontal lines indicate a statistically significant difference with the two indicated conditions. Ctrl, control; TM, tunicamycin; TG, thapsigargin (0.5 µM); N, nucleus.

ACCEPTED MANUSCRIPT

Figure 4: TM-induced ER stress marker induction is not blocked by HDLs

A. MIN6 cells were left untreated (C) or treated with 2 µg/ml TM during 6 hours (panels A, C and D) or 24 hours (panels B and E) in the presence or in the absence of 1 mM HDLs. The cells were then lysed and RNA and proteins were isolated. The extent of XBP1 mRNA splicing was then determined (panel A). The pound sign indicates an unspecific band (Petremand et al., 2012). Western blot analyses were performed to assess protein expression of BiP (panel B), phospho-PERK (panel C), and CHOP (panel E). CHOP mRNA expression was determined by quantitative PCR (panel D). The results shown in panels A to E are derived from 4, 6, 4, 6, and 5 independent experiments, respectively. Asterisks denote statistically significant difference between the indicated conditions; NS, not significant.

Figure 5: HDLs do not restore TM-induced folding and trafficking impairment

MIN6 cells were infected with VSVG-GFP-encoding lentiviruses and treated two days later with or without 2 µg/ml TM in the presence or in the absence of 1 mM HDLs for 5 hours at 40°C. The cells were then incubated or not for an additional 1 hour time period at 32°C. Immuno-cytochemistry was performed on non-permeabilized cells using an antibody directed against the ectopic part of VSVG (left-hand side of the figure) and on permeabilized cells using an antibody recognizing the correctly folded form of the protein (right-hand side of the figure). The percentage of cells expressing cell surface or folded VSVG was quantitated and shown in the bar graphs (4 independent experiments). Asterisks denote statistically significant difference between the indicated conditions; NS, not significant.

Figure 6: Effect of HDLs on Akt and JNK activity in the presence of various ER stressors

MIN6 cells were left untreated (Ctrl) or stimulated with 0.5 µM TG for 6 hours, 2 µg/ml TM for 12 hours, a cocktail of inflammatory cytokines (IL1β IFNγ, and TNFα each at a 1'000 U/ml concentration) for 8 hours, and 0.3 mM palmitate/0.5% BSA for 24 hours, in the presence or in the absence of 1 mM HDL. **A.** Apoptosis was then measured by scoring the percentage of cells with pycnotic or fragmented nucleus. **B-C.** Alternatively, the cells were lysed and activation of Akt (panel B) and JNK (panel C) was assessed by Western blotting using an antibody recognizing Akt phosphorylated on serine 473 and an antibody specific for the active phosphorylated forms of JNKs. The blots were reprobed with antibodies recognizing total Akt

ACCEPTED MANUSCRIPT

and total JNK. The intensities of the phosphorylated bands were normalized against those of total Akt and total JNK and further normalized to the control condition. The results are derived from 3-6 independent experiments. Asterisks indicate a statistically significant difference between the indicated conditions.

Figure 7: HDLs protect Min6 cells at sub-micromolar concentrations

MIN6 cells were left untreated (Ctrl), incubated with 1 mM HDL, or stimulated with 2 µg/ml TM or 0.5 µM TG in the presence of increasing concentrations of HDLs. Apoptosis was then measured 24 hours later by scoring the percentage of cells with pycnotic or fragmented nucleus (3 independent experiments). Asterisks indicate a statistically significant difference between apoptosis induced by TM or TG alone and the indicated conditions.

Figure 8: HDLs protect beta cells at several levels along ER stress-mediated apoptosis pathways

HDLs have the capacity to preserve the morphology of the ER in presence of various ER stressors. In some cases (TG, palmitate), this is associated with a maintenance of ER functionality (protein folding, protein trafficking through the ER), which is required for the ability of HDLs to blunt the UPR and to efficiently protect the beta cells (Petremand et al., 2012). In other cases (TM), preservation of the ER morphology is not associated with maintenance of the ER functionality and inhibition of the UPR. Nevertheless, in these situations, HDLs can still inhibit apoptosis downstream of the UPR (present study). Therefore HDLs have the capacity to activate several, apparently non-redundant, anti-apoptotic pathways in beta cells, which might explain their ability to protect beta cells in response to a variety of insults.

ACCEPTED MANUSCRIPT

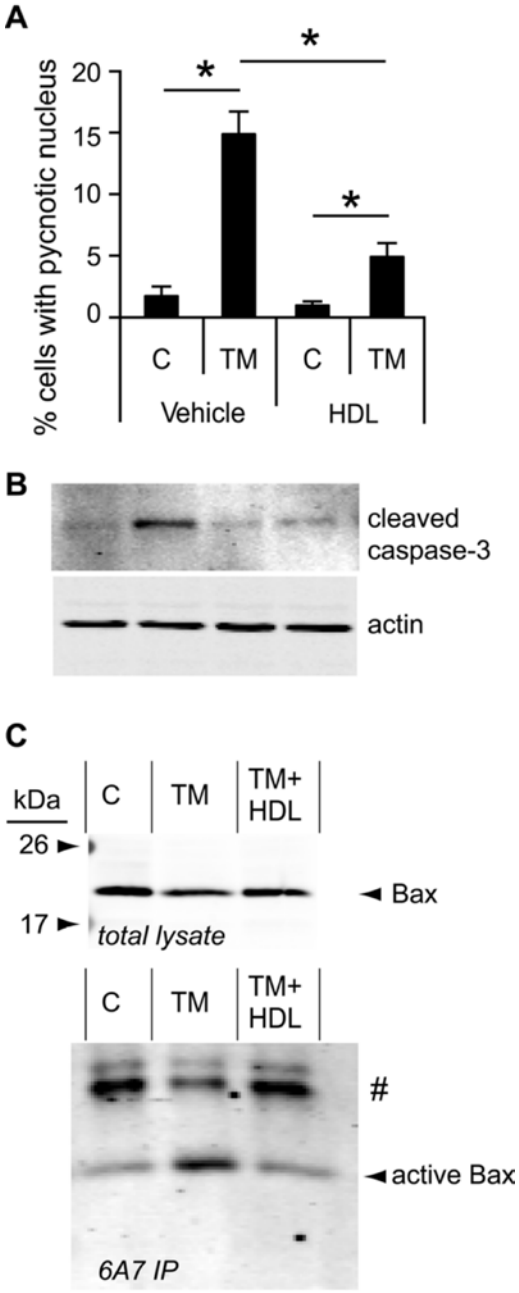

Figure 1

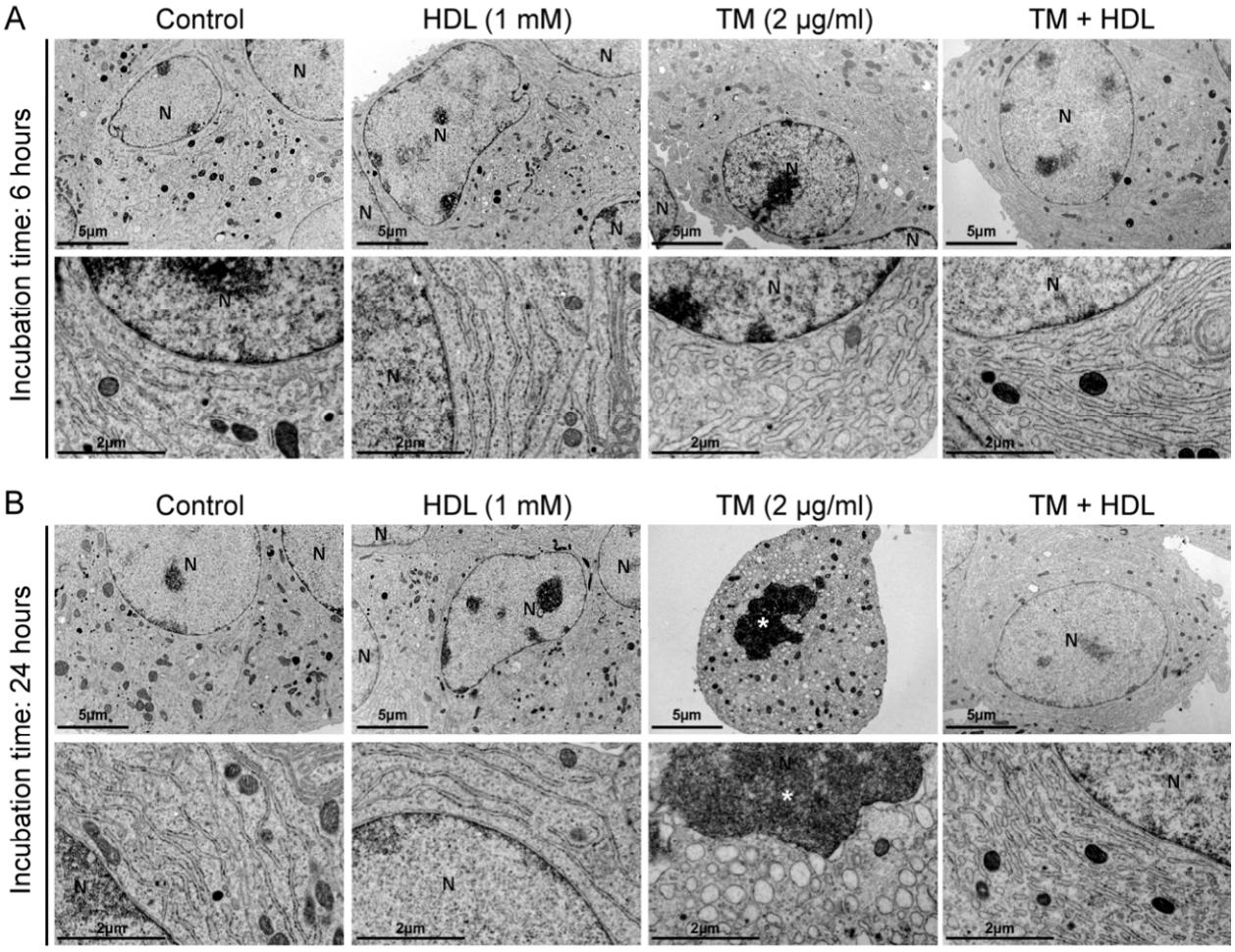
A
Control
HDL (1 mM)
TM (2 µg/ml)
TM + HDL
Incubation time: 6 hours
B
Control
HDL (1 mM)
TM (2 µg/ml)
TM + HDL
Incubation time: 24 hours
N
5µm
2µm
*

Figure 2

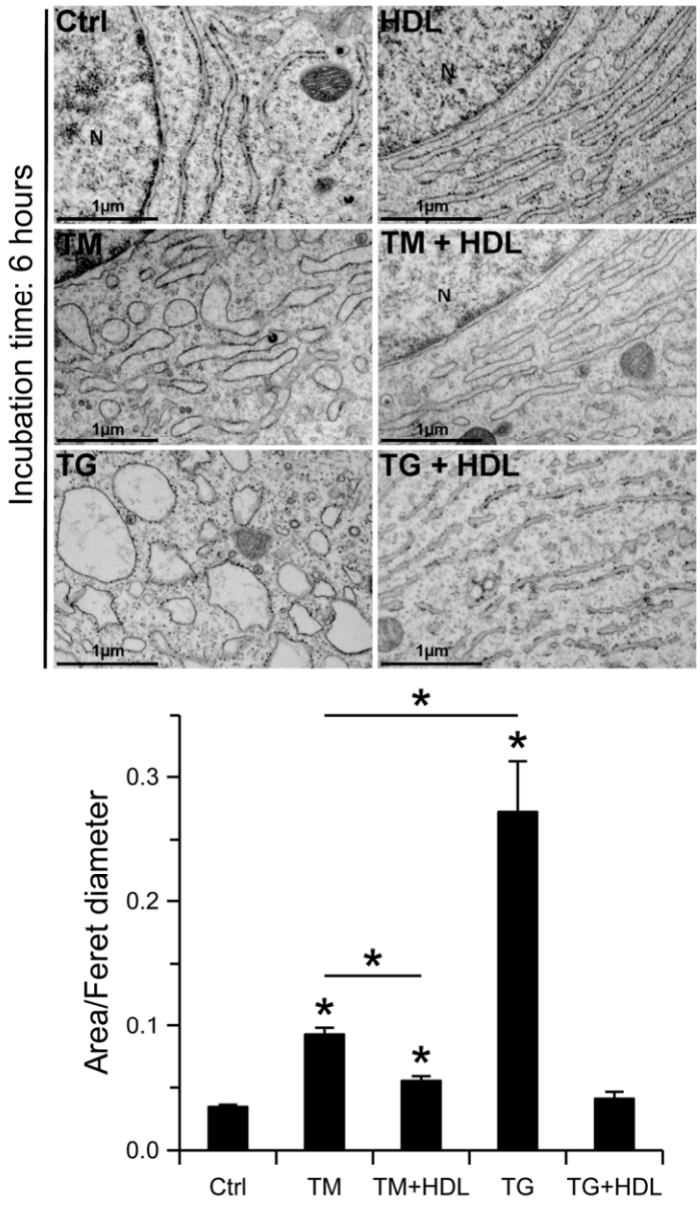
Incubation time: 6 hours
Ctrl
HDL
TM
TM + HDL
TG
TG + HDL
N
1µm
Area/Feret diameter
0.0
0.1
0.2
0.3
Ctrl
TM
TM+HDL
TG
TG+HDL
*

Figure 3

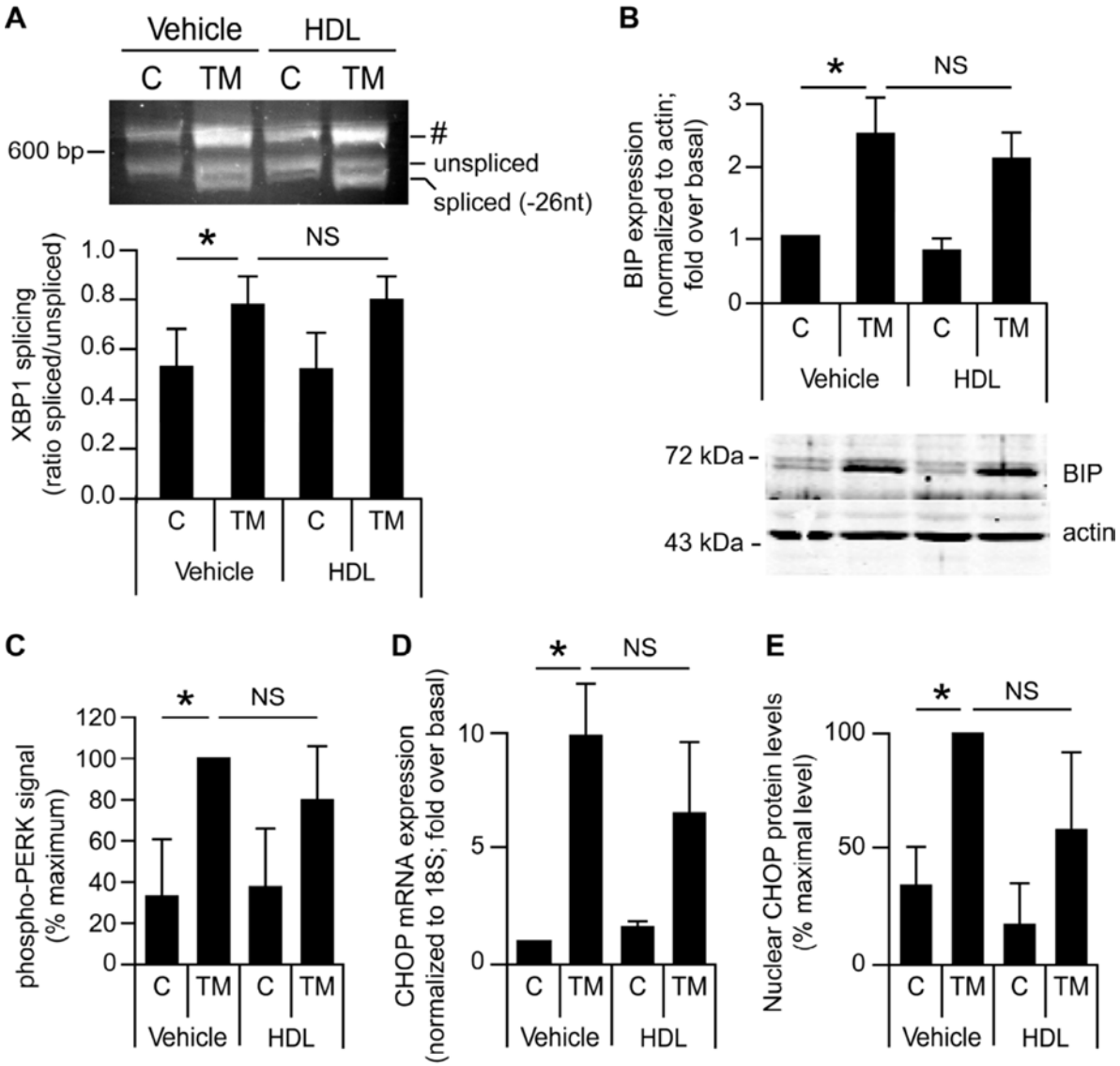
A
Vehicle
HDL
C
TM
C
TM
600 bp
#
unspliced
spliced (-26nt)
XBP1 splicing
(ratio spliced/unspliced)
1.0
0.8
0.6
0.4
0.2
0.0
*
NS
C
TM
C
TM
Vehicle
HDL
B
BIP expression
(normalized to actin;
fold over basal)
3
2
1
0
*
NS
C
TM
C
TM
Vehicle
HDL
72 kDa
BIP
43 kDa
actin
C
phospho-PERK signal
(% maximum)
120
100
80
60
40
20
0
*
NS
C
TM
C
TM
Vehicle
HDL
D
CHOP mRNA expression
(normalized to 18S; fold over basal)
10
5
0
*
NS
C
TM
C
TM
Vehicle
HDL
E
Nuclear CHOP protein levels
(% maximal level)
100
50
0
*
NS
C
TM
C
TM
Vehicle
HDL

Figure 4

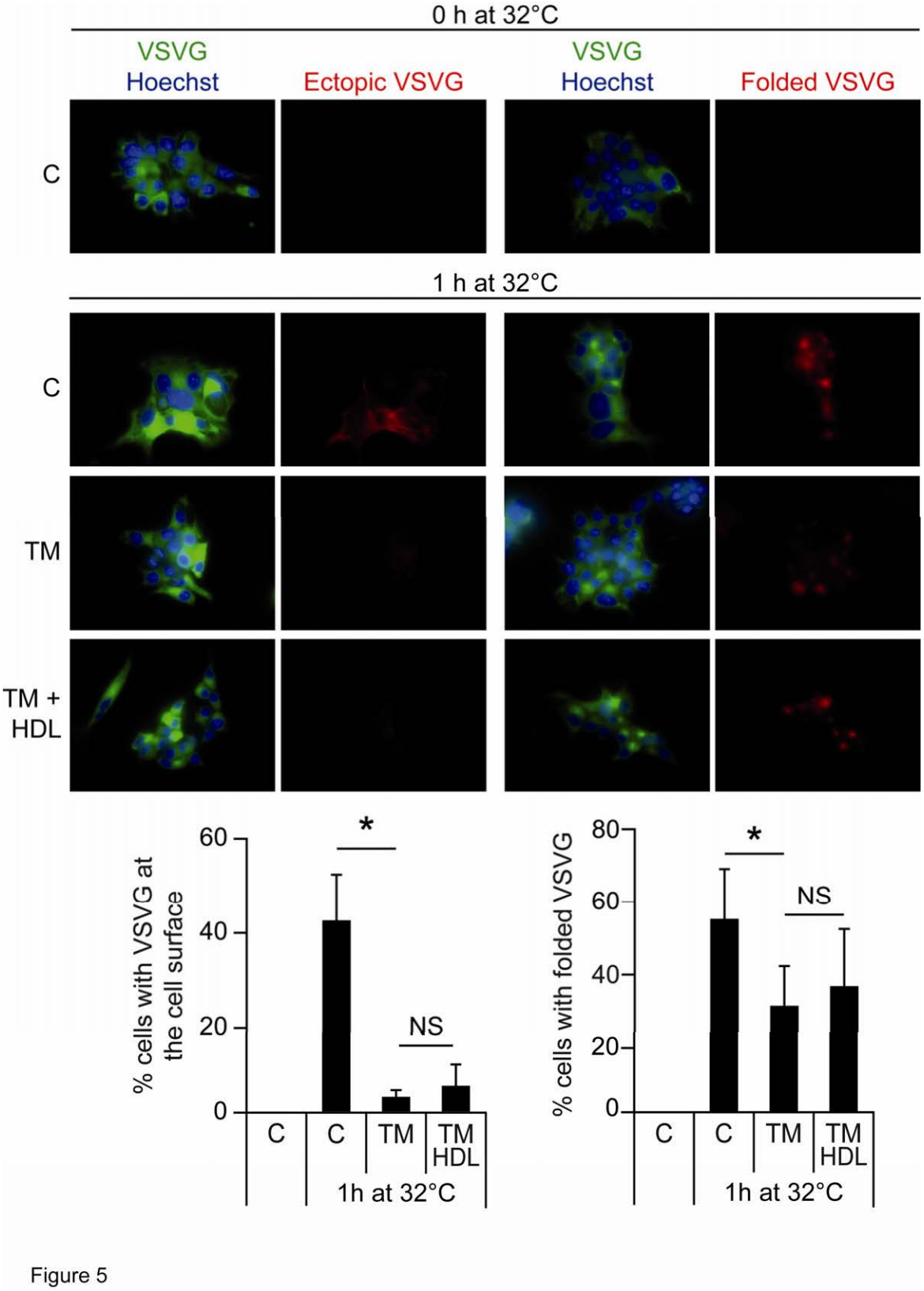
0 h at 32°C
VSVG
Hoechst
Ectopic VSVG
VSVG
Hoechst
Folded VSVG
C
1 h at 32°C
C
TM
TM +
HDL
% cells with VSVG at
the cell surface
60
40
20
0
*
NS
C
C
TM
TM
HDL
1h at 32°C
% cells with folded VSVG
80
60
40
20
0
*
NS
C
C
TM
TM
HDL
1h at 32°C

Figure 5

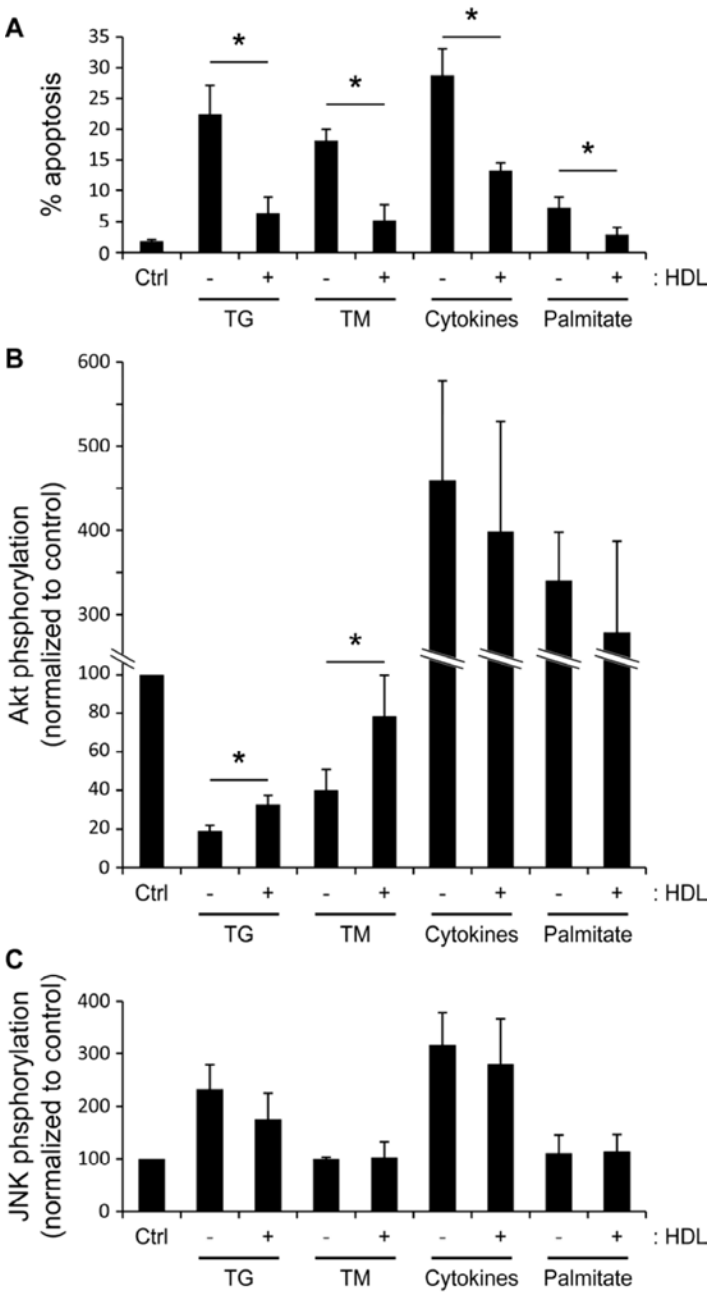
A
% apoptosis
35
30
25
20
15
10
5
0
*
*
*
*
Ctrl
-
+
-
+
-
+
-
+
: HDL
TG
TM
Cytokines
Palmitate
B
Akt phsphorylation
(normalized to control)
600
500
400
300
100
80
60
40
20
0
*
*
Ctrl
-
+
-
+
-
+
-
+
: HDL
TG
TM
Cytokines
Palmitate
C
JNK phsphorylation
(normalized to control)
400
300
200
100
0
Ctrl
-
+
-
+
-
+
-
+
: HDL
TG
TM
Cytokines
Palmitate

Figure 6

ACCEPTED MANUSCRIPT

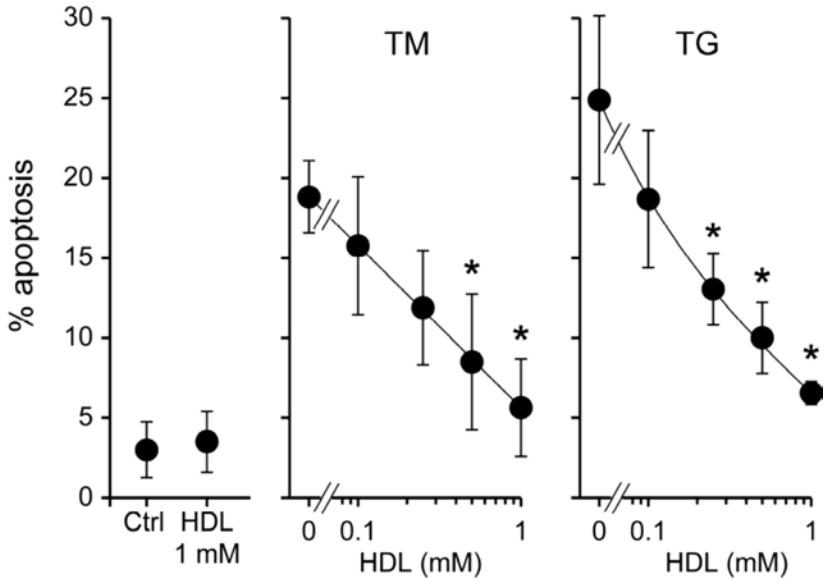

Figure 7

ACCEPTED MANUSCRIPT

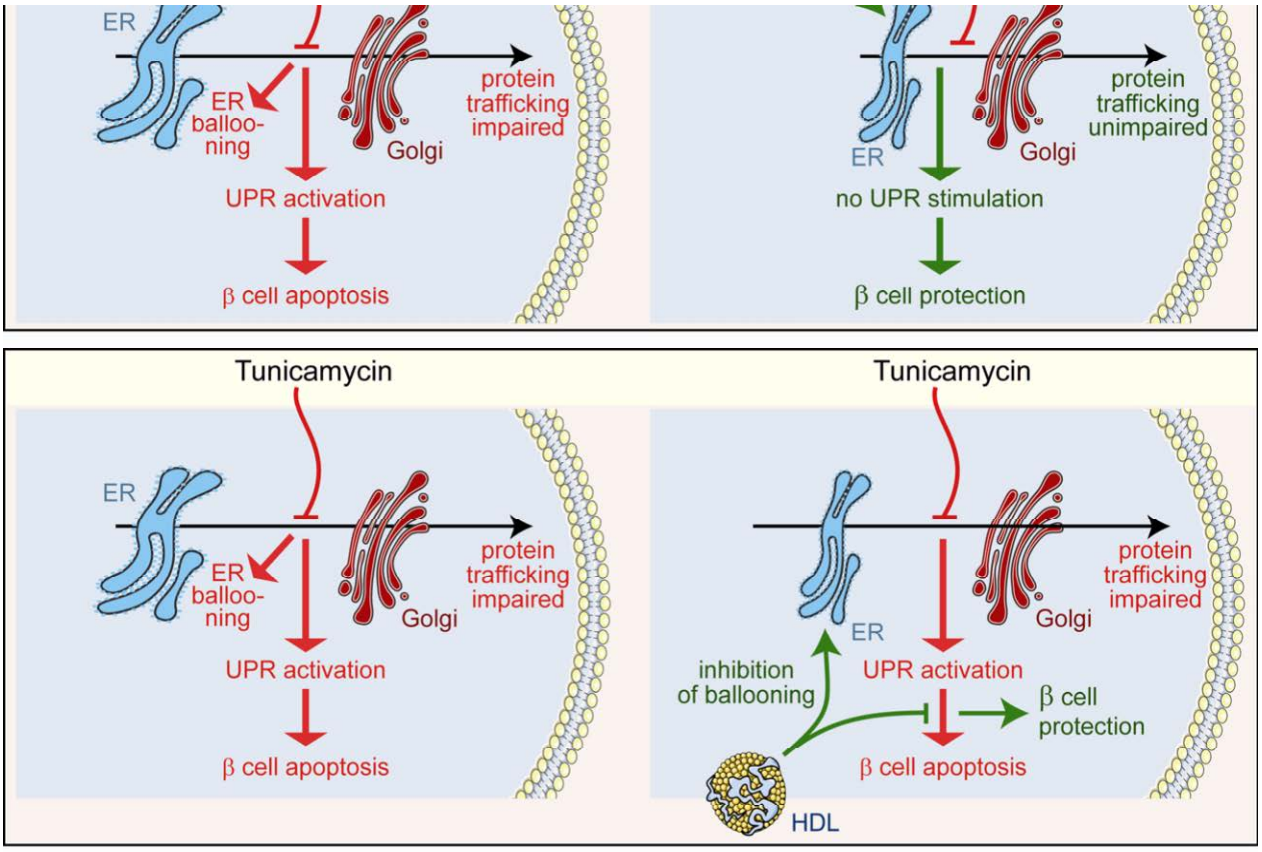

Figure 8